

RADIO-CLINICAL AND ANATOMOPATHOLOGICAL OCCURRENCE OF NEPHROBLASTOMA MANAGED AT THE UNIVERSITY CLINICS OF KINSHASA

Frederick Tshibusu Tshienda^{1}, Oscar Mokambo Eputa^{1*}, Nina Doma Nsimba², Aléine Budiongo Nzazi², Angèle Mbongo Tanzania¹, François Beya Kabongo³, Karim Assani², GuethKundabiAkoto², Damien Kamate Kiraulu⁴, Valentin Kazadi Tshipamba⁴, Theo Mbala Biayi⁴, Nestor Ntumba Kabeya⁴, Idesbald Mwepu⁴, Jean-Pierre Bungu Kalala⁴, Bejamin Kabwe Mwilambwe⁵, Bienvenu Lebwaze Massamba³, Jean Mukaya Tshibola¹, Michel Lelo Tshikwela¹, Antoine Molua Aundu¹, René Ngiyulu Makwala²*

Division of Diagnostic Imaging, Kinshasa University Hospital, School of Medicine, University of Kinshasa, Kinshasa, Democratic Republic of the Congo

Department of Anatomopathology, Kinshasa University Hospital, School of Medicine, University of Kinshasa, Democratic Republic of the Congo

Department of Surgery, Division of Pediatrics, Kinshasa University Hospital, School of Medicine, University of Kinshasa, Democratic Republic of the Congo

Department of Anesthesia and Intensive Care, Kinshasa University Hospital, School of Medicine, University of Kinshasa, Kinshasa, Democratic Republic of Congo.

Summary: OBJECTIVE: To establish the radio-clinical and anatomopathological occurrence of nephroblastoma treated at the University Clinics of Kinshasa. **MATERIALS AND METHODS:** This was a descriptive, documentary study of 45 patients followed up for renal mass syndrome diagnosed by ultrasonography and supplemented by CT scan and chest X-ray at the University Clinics of Kinshasa during a six-year period from 2016 to 2021. A Phillips U-22 ultrasound scanner, an Eclon Hitachi scanner and a Siemens digital X-ray machine were used.

RESULTS: We noted a male predominance with a sex ratio of 2H/1F; the median age of patients was 3 years with extremes ranging from 2 months to 10 years. The clinic was dominated by palpation of an abdominal mass in 71.1% of cases. The majority of the tumors were solid-heterogeneous in 55.2%. The left renal localization was predominant in 51.2% of cases. Ultrasonography was the imaging modality used for diagnosis. Computed tomography (CT) and chest radiography were the imaging modalities used for the assessment of loco-regional and distant extension in search of pulmonary metastases. Stages I and III were predominant in 78.6% of cases, mixed type nephroblastoma represented 55.1% of cases and intermediate risk tumors 85.7% of cases.

CONCLUSION: The clinico-radiological profile of nephroblastoma in Congolese children was more revealed by an abdominal mass [71.1%], found in patients aged 2 to 240 months with a male predominance. The most predominant sonographic appearance was that of a solid, heterogeneous tumor [55.2%] and the left renal location was the most predominant [51.2%]. Stages I and III were predominant [78.6%] of cases. Mixed-type nephroblastoma represented 55.1% of cases and intermediate-risk tumors 85.7% of cases. These observations corroborate the majority of the data in the literature.

KEYWORDS: radio-clinical occurrence Nephroblastoma anatomopathology

INTRODUCTION

Nephroblastoma, or Wilms' tumor, is a renal tumor that occurs predominantly in children. It accounts for more than 90% of malignant renal tumors in children and affects mainly children under 5 years of age [1-3]. Nephroblastoma is very different from adult kidney cancer, as it is an embryonic tumor, developing from the metanephros, whose differentiation and proliferation give rise to the kidney [3]. In most Western

populations, nephroblastoma accounts for up to 6% of all cancers diagnosed in children. In black populations in North America and Africa, the proportion is about 10% [4]. It is rarely found in adults [5,6]. In francophone sub-Saharan Africa, nephroblastoma is among the five diseases that account for 70% of childhood cancers [7]. Although Wilms' tumor is often curable in developed countries, affected children in resource-limited areas of sub-Saharan Africa experience poor outcomes. Abdallah FK et al(9) in a 2001 analysis of nephroblastoma survival in Kenyan patients reported a two-year event-free survival (EFS) of only 34.7% [8], which contrasts with survival rates exceeding 90% at 5 years in developed countries. However, thanks to the Franco-African Pediatric Oncology Group (FAOPG), a protocol better suited to the setting where patients are seen late with a large abdominal mass, the prognosis has improved considerably in Francophone Africa [7,9]. Imaging has a key role in the management of renal tumors in children, since the therapeutic decision to institute preoperative chemotherapy in nephroblastoma in children is made without anatomopathological evidence, according to the protocol of the International Society of Pediatric Oncology (SIOP) 2001 [2,10]. A study carried out in the pediatric oncology unit of Bamako, by Abdoul KD et al [9] in Mali, reports that nephroblastoma occupies the third place (15%), of pediatric cancer after non-Hodgkin's malignant lymphomas and retinoblastoma. En République Démocratique du Congo (RDC), déjà dans les années 80 et 90, les études de Mputu[11], de Luntala[12], de Kongolo [13], de Palangi [[14] et de Kazadi [15] avaient démontré que cette pathologie grave est fréquente dans notre milieu où il poses a real problem of early diagnosis. Recently, a literature review of cases in the pediatric hemato-oncology unit of CUK from 2000 to 2018 had reported a rate of 13% of cases of nephroblastoma, placing it in 4th position after retinoblastoma, lymphomas and leukemias [16]. If some studies evaluating the frequency of nephroblastoma on the basis of conventional radiology data have already been carried out [10], few studies have evaluated the clinical, radiological and anatomopathological profile of nephroblastoma in the hospital environment of Kinshasa; for this reason, we propose to establish the radio-clinical and anatomopathological occurrence of nephroblastoma taken in charge at the University Clinics of Kinshasa.

MATERIALS AND METHODS

Type and period of study: This is a descriptive documentary study of nephroblastoma cases followed up at the CUK for a period of six years, i.e. from January 2016 to January 2021. Several services contributed to the management of these patients, including the Pediatric Oncology Unit, the Medical Imaging Service, the Pediatric Surgery Service, the Department of Pathological Anatomy and the Department of Medical Biology. **Study population:** this study included 45 patients, aged from 1.5 months to 10 years with a median age of 3.0 with extremes (2.0-4.0) years. Of the 45 patients, 30 were male and 15 were female. **Inclusion criteria:** Any patient who consulted for an ultrasonographically confirmed renal mass and who had a chest X-ray and/or CT scan as part of the extension work-up. **Non-inclusion criteria:** The following were not included in this study: patients who did not perform the above-mentioned imaging modalities, patients who did not perform histopathological examinations and/or patients with incomplete medical records. **Parameters of Interest and Operational Definitions:** Sociodemographic parameters included patient age and gender. Regarding clinical parameters, we noted: palpated abdominal mass, hematuria, abdominal pain, alteration of general condition, digestive disorder and abdominal trauma. As biological parameters; we analyzed: hemoglobin, urea and creatinine. **The ultrasonographic parameters:** the ultrasonographic analyses carried out, before any therapeutic management were considered: the tumor characteristics below: the right, left or bilateral localization of the tumor; the renal take-off point (superior pole, inferior pole, medio renal, toto renal); the tumor volume, obtained by an automatic calculation starting from three dimensions below: height (h) x width (w) x thickness (e) x 0.523 ,the product expressed in cm³ and in ml; the echostructure: which can be solid (homogeneous or heterogeneous) or mixed (solid-cystic) and or cystic; the difference between necrotic and cystic areas being more realized according to their shape, if it was fluid patches, poorly delimited, they were then considered as necrotic, if they were rounded patches, well limited, of cysts. the presence or not of the tumor capsule (capsule being a layer that separates the mass from the surrounding structures); the echogenicity of the tumor (the brightness or not of the tumor in relation to the surrounding structures, which can be hypoechoic, hyperechoic and or isoechoic; the spur sign : which is the extension of the healthy renal parenchyma progressively connecting to the mass, the regular or irregular contours of the tumor; the suspicion of tumor rupture in front of a perirenal or peri-tumoral collection, the presence of calcifications (intra-tumoral hyperechoic images), the repression of the pyelocalic cavities and or vessels, the compensatory hypertrophy of the contralateral kidney, the tumor vascularization. Other parameters were

evaluated, among others the loco-regional tumor extension, which consisted in evaluating: the permeability of the renal vein and the inferior vena cava by the presence or not of a thrombus, the transmedian extension, the median line being defined by the white line, the presence : intraperitoneal effusion, satellite nodule on the homolateral kidney, nodule to the contralateral kidney, adenomegaly , or liver metastases. The CT parameters investigated were the following: general characteristics of the tumor including: tumor volume: height (h) x width (w) x thickness (e) x 0.523, expressed in cm³ and or ml; the spur sign defined as the extension of healthy renal parenchyma progressively connecting to the mass, the presence or not of the tumor capsule, the tumor homogeneity, the spontaneous density of the tumor, the presence of calcifications, cystic, necrotic and/or hemorrhagic areas, the enhancement after injection of the contrast medium, the tumor extension defined by: infiltration of the perirenal fat, loss of the peri-tumoral fat border: defined by the absence of fatty border between the tumor and the perirenal structures (muscle, liver, or spleen according to laterality, diaphragm, pancreas), suspicion of tumor rupture in front of a perirenal hematoma with important perirenal fat infiltration, crossing of the patient's midline by the tumor, the median line being defined by the line of the vertebral spinous veins, the permeability after injection of the renal vein and the inferior vena cava (IVC), the presence of the nodule in the homolateral kidney, adenomegaly, intraperitoneal liquid effusion, metastatic hepatic extension or by contiguity .The parameters investigated on the chest X-ray were: pulmonary metastases that could be manifested as nodular opacity, pleural effusion and nodular thickening of the axial interstitium in the context of carcinomatous lymphangitis. The anatomopathological parameters investigated were: the histological type of the tumor (epithelial, stromal, blastematosus, mixed, with focal anaplasia and with diffuse anaplasia), the prognostic groups (low risk, intermediate risk and high risk) as well as the stages according to the 2001 SIOP classification. Finally, the grouping of four stages into two major groups among others: stages I and II: considered as tumors with complete resection and stages III and IV considered as tumors with incomplete resection according to the ultrasonographic characteristics.As for data processing and statistical analysis, it should be noted that the data were collected on a data collection form encoded using Excel 2013 software. After verification and cleaning of the database, they were exported to SPSS for Windows version 24 for analysis. Categorical variables were presented as absolute and relative frequencies (%), quantitative variables were summarized by measures of central tendency and dispersion. The mean and its standard deviation were reported for data with a Gaussian distribution; however, those that did not follow the Gaussian distribution were summarized as median and interquartile range (IQR). Pearson's chi-square or Fischer's exact test was used to compare proportions; Student's t-test compared means; and Mann Whitney U-test compared medians. For all tests used, the p value < 0.05 was the threshold of statistical significance.**RESULTS:** In relation to the socio-demographic parameters; the median age in the present study was three years with the extremes ranging from two months to ten years [figure 1]. The majority of patients were between two and four years of age (44.4%) [Figure 1]. The majority of patients were male (66.7%) with a sex ratio of 2:1 [Figure 2]. The median values of urea and creatinine were 20.8 (13.4-27.1) mg/dl for urea and 0.60 (0.45-0.70) mg/dl for creatinine. The overall mean hemoglobin value was 8.5±1.9 g/dl [Table 1]. The analysis of the ultrasonographic parameters, reveals the use of this technique in forty three patients, that is to say 95.6%. Among these forty-three patients, we found twenty-two tumors in the left kidney, i.e. 51.2%, nineteen tumors in the right kidney, i.e. 44.2%, and a bilateral localization in two patients, i.e. 4.7% [table 2].The majority of tumors had a heterogeneous solid echostructure in twenty-four patients, i.e. 55.8%; solid tumors with necrotic-cystic patches were present in nineteen patients, i.e. 44.2% [Table 2] . The analysis of flight points revealed the following findings: nineteen tumors were superior polar, i.e. 44.2%, eleven inferior polar tumors, i.e. 25.6%, one medio-polar tumor, i.e. 2.3% and twelve total renal tumors, i.e. 27.9% [table 2]. The median value of tumor volume was 985 (665-1196) ml with the extremes ranging from 100 ml to 6127ml. The spur sign was found in twelve patients or 27.9%. The tumor contours were irregular in thirty patients ,i.e. 69.8% and regular in thirteen patients ,i.e. 31.2% %[table 2]. The tumor capsule was intact in eighteen patients, i.e. 41.9%, while tumor rupture was found in three patients, i.e. 7% [table 2]. The pyelocalic cavities were compressed in four patients, i.e. 9.3% [table 2]. In the whole group, there were twenty-three hypoechoic tumors, i.e. 53.5%. In the boys, twelve patients (42.9%) had hypoechoic tumors, whereas in the girls eleven patients had hypoechoic tumors [Table 2]. Hyperechoic tumors were found in twelve patients, i.e. 27.9%; in boys nine patients, i.e. 32.1% and in girls three patients, i.e. 20% and iso echogenic tumors in eight patients, seven boys and one girl. We found intratumoral calcifications in nine patients, i.e. 20.9% [Table 2]. Compensatory hypertrophy of the contralateral kidney was noted in four patients, i.e. 9.3%, and tumor vascularization was

well objectified in seventeen patients, i.e. 39.5% [table 2]. The inventory of the parameters of locoregional tumor extension at ultrasonography reveals the following; the reflow without invasion of the neighboring structures was found in seventeen patients, i.e. 39.5%; adenomegaly was found in thirteen patients, i.e. 30.2% [table 2]. The venous thrombus was found in twelve patients, i.e. 27.9%, in five patients, i.e. 11.6%, the thrombus was located in the renal vein and in seven patients, i.e. 16.3%, the thrombus was located in the inferior vena cava [table 2]. In seven patients (16.3%) we found a transmedian extension. Peritoneal effusion was found in five patients (11.6%) and liver metastases in three patients (7%). The entire group had a median tumor volume value of 560.6 (313.9- 843.4) ml. The spur sign was found in four patients% [Table 2]. Tumor capsule was noted in two patients. Tumor homogeneity was marked by five homogeneous tumors, three heterogeneous tumors and one mixed tumor [Table 2]. Tumor enhancement was present in six patients; perirenal fatty infiltration, midline crossing, pathological lymph nodes, intraperitoneal effusion and pulmonary metastases were found in one patient each % [table 2]. The study of the CT parameters reveals that CT scan was performed in only nine patients, i.e. 20%, including two patients who did not perform the diagnostic ultrasound scan % [table 2]. Chest radiography had diagnosed pulmonary metastases in six patients, i.e. 13.3%, of which five patients with nodular metastases and one patient with the pleuro-liquid metastatic form. On the anatomopathological level, twenty nine patients, or 64.4%, had undergone histopathological examination after an enlarged total uretero-nephrectomy, among whom we note seventeen boys and twelve girls [table 2]. Nephroblastoma was confirmed in twenty seven patients, i.e. 93.1%, including fifteen boys and twelve girls [table 2]. The other two patients (6.9%) in whom nephroblastoma was not histopathologically confirmed, presented with congenital mesoblastic nephroma or Bolande's tumor, diagnosed at 4 months for one patient, and an inflammatory mass, diagnosed at 8 years for the other patient [Table 2]. According to the histological types, sixteen patients (55.1%) had the mixed type; the stromal and regressive types were found in 3 patients (10.3% each); the blastomatous and epithelial types were found in 2 patients each [Table 3]. [Table 3]. We also noted 3 patients one of which had a partially differentiated cystic nephroblastoma, another had a congenital mesoblastic nephroma and the last one had an inflammatory mass [Table 3]. According to the tumor stage; stages I and III were in the majority, representing 39.3% each; while stage II represented 17.9% and stage IV 3.6% [Figure 3]. We noted 85.7% of tumors of intermediate risk against 7.1% of low and high risk tumors in the same proportions [Table 3]. According to the ultrasonographic characteristics of the tumors; we noted in the right kidney 11 tumors, that is 68.8% of complete resection and 2 tumors, that is 20% of incomplete resection while in the left kidney contained 5 tumors, that is 31.3% of complete resection and 8 tumors, that is 80% of incomplete resection [Table 4]. The difference was statistically significant ($p=0.021$). There were 7 tumors, or 43.8% of complete resection with irregular contours and 7 tumors, or 70% of incomplete resection. On the other hand, 9 cases of tumors with regular contours, i.e. 56.3% of complete resection, against 3 cases, i.e. 30% of incomplete resection [Table 4]. The difference was statistically significant ($p=0.014$). There was one tumor with complete resection and calcifications; while 7 tumors, or 70% of incomplete resection with calcifications [Table 4]. The difference was statistically significant ($p=0.001$). Taking into account the ultrasound elements of tumor extension according to stage, we found 2 tumors, or 12.5% of complete resection with extension beyond the midline and 3 tumors, or 30% of incomplete resection with extension beyond the midline [Table 4]. Among the tumors that were displacing neighboring structures, 6 (37.5%) had complete resection, while 7 (70%) had incomplete resection [Table 4]. The difference was statistically insignificant ($p=0.092$). We noted one tumor with complete resection and intraperitoneal effusion; while 3 tumors, or 30%, had intraperitoneal effusion and incomplete resection [Table 4]. The difference was statistically insignificant ($p=0.142$). In addition, 4 completely resected tumors, i.e. 25%, had renal venous thrombosis, while 2 incompletely resected tumors, i.e. 20%, had venous-cavity thrombosis [Table 4]. The difference was statistically insignificant ($p=0.677$). For patients with adenomegaly, we found 6 tumors, or 37.5% completely resected; while 4 tumors, or 40% incompletely resected [Table 4]. The difference was statistically insignificant ($p=0.609$). We noted 2 patients with liver metastases, all of whom had incompletely resected tumors [Table 4 and Figure 3.A].

DISCUSSION: In our series, the median age in the study population was 3 years with extremes ranging from 2 months to 10 years. The majority of patients were between 2 and 4 years of age, representing 44.4% of cases. Diakite F et al [17] and Atanda AT et al [18] in Guinea (2012) and Nigeria (2015) respectively had found a mean age of about 5 years. The extremes of age ranged from 13 months to 13 years in the study of Diakite et al [17]. This difference could be explained by the improvement of the management with the support of GFAOP. Molua [1] had noted the extremes of age 1 and 5 years. This is consistent with our

observation and those of several authors [2,9,10,19]. In the present study, the male sex was more affected than the female sex, i.e. 30/15 with a sex ratio of 2/1. Kante A. et al [20] noted a slight female predominance. Our observation is similar to those of Atanda AT et al [18] and Diakite F et al [17], but no statistically significant association was demonstrated. In our series; clinical signs were dominated by the discovery of an abdominal mass reported by the parents (71.1%), followed by general signs (44.4%), palpated abdominal mass (35.6%), abdominal pain (31.1%), hematuria (24.4%), constipation (2.2%) and trauma (2.2%). These results are similar to those of Bouzhir AM et al [21]. According to data from the National Cancer Institute in the USA [21], asymptomatic abdominal distension : constitutes the most frequent clinical presentation discovered in a child during bathing or dressing, abdominal pain is seen in 40% of cases; macroscopic hematuria is seen in 18% of patients as a clinical presentation and microscopic hematuria is present in 24% of cases, arterial hypertension is present in almost 25% of patients at the time of discovery of nephroblastoma, and is secondary to activation of the renin-angiotensin-aldosterone system. Symptoms of altered general condition, such as anorexia, weight loss and fever, may occur in less than 10% of cases. Other manifestations related to complications may also be indicative of nephroblastoma, including vascular obstruction or metastases, including pulmonary symptoms due to pulmonary metastases, abdominal pain due to liver metastases, collateral venous circulation, or varicoceles due to obstruction of the inferior vena cava. Pulmonary embolism (rare). The renal function studied by the determination of urea and plasma creatinine was normal in our study. This could be explained by the unilaterality of the renal involvement. In fact, in case of bilateral damage, we think that the rest of the healthy parenchyma retains function. These data agree with those of Molua [1] and those of the literature. Our study did not note any cases of congenital malformation or syndromes predisposing to nephroblastoma. Bouzhir MA et al. Bouzhir MA et al [21] noted that abdominal ultrasound performed in all patients (100% of cases) showed a slight predominance of right renal tumors, i.e. 50% and left renal tumors 46.7% of cases, while bilateral involvement 3.3% of cases. Our observations are similar to those of Diakite F et al [17]. In our series, abdomino-pelvic ultrasound was performed in 95.6%, i.e. 43/45. It showed a right kidney tumor in 19 cases (44.2%), and a slight predominance of left kidney tumor in 22 cases (51.2%), i.e. unilateral involvement in 95.4%, and bilateral in 2 cases (4.7%). One of 2 cases of bilateral tumor had 2 to 3 intra-renal nodules and ultrasound had hypothesized nephroblastomatous lesions. However, these 2 cases had no histopathologic evidence. In some previous studies (LAIGLE V. et al in Nantes in 2011), tumor heterogeneity on ultrasound was a discriminating feature, nephroblastoma being more heterogeneous than other renal tumors, but this data remained at the limit of significance ($p=0.05$) and was not confirmed on CT. In our study, the majority of the tumors had a solid and heterogeneous echostructure in 55.8% of the cases but we could not analyze the discriminating characteristics of nephroblastoma because the number of other non-nephroblastoma tumors was insufficient (only 2 cases including a mesoblastic nephroma and an inflammatory mass). According to the literature, nephroblastoma usually develops at one renal pole but can also be multifocal, disorganizing and displacing normal anatomical elements of the kidney [23,24]. This corroborates our study which shows that 19 cases (44.2%) were superior polar, 11 cases (25.6%) inferior polar i.e. a frequency of 69.8% of polar development, 1 case (2.3%) mid-renal and 12 cases (27.9%) occupied the entire renal parenchyma. Zrig A. et al [25] in Tunisia in 2014 had found the spur sign in 45 patients out of 113 observations or 39.8%. While in our series, this sign represented 27.9% (12cas); this low rate may be attributed to the large width of the tumor. In most cases, the mass is well limited [23], whereas in our series, we found masses with irregular contours in 69.8% (30 cases). This high rate of irregular contours could be justified by the initial ultrasound performed at an advanced stage of the tumor. The mass may appear encapsulated [23], in our series we found 41.9% (18 cases) of encapsulated tumor and this could be related to the local stage of the mass (stage I and II and III) which is determined after nephrectomy and histopathological analyses. Most of the tumors were hypoechoic in 53.5% (23cas), hyperechoic tumors in 27.9% (12cas) and iso echogenic in 18.6% (8cas); hypoechoic masses were more noticed in girls, hyper and iso echogenic more noticed in boys with significant statistical analysis ($p=0.037$). However, this data is subject to the small sample size of our study and thus opens up a boulevard for future research that can confirm or refute. Calcifications are possible in renal tumors but not very frequent. They help especially, associated with the corbelling sign, the invasion of the medullary canal (on CT) and the forward displacement of the aorta in the differential diagnosis with neuroblastoma [2]. In our series, we found nine lesions with calcifications (20.9%), arguing in favor of an advanced stage tumor (III or IV); therefore an incompletely resected tumor with a statistically significant analysis ($p=0.001$). In relation to locoregional

extension: venous thrombosis is classically described as a sign pointing to nephroblastoma; LAIGLE et al [2] found 4 cases of nephroblastoma, two of the tumors were non-nephroblastoma, 6 cases (10%) out of 60 and the 2 cases were false negatives on ultrasonography and thrombosis was present on CT. In our series, we found 12 patients with venous thrombosis out of 43 or 27.9%; among them, 5 patients had benefited from histopathological analysis after nephrectomy, the diagnosis of nephroblastoma was confirmed. The high rate of venous thrombosis in this study could be justified by the late discovery of the tumor on the one hand and by the ability of the radiologist to look for the latter before any case of nephroblastoma. According to the literature [2], it is known that it is possible to find large reaction or stasis lymph nodes, without tumor invasion, which are responsible for false positives. During the operation, the surgeon has no intraoperative morphological criteria to differentiate metastatic adenopathy from reactive adenopathy. Only histological data can determine this difference, which is why the SIOP recommends systematic biopsies. However, their absence could be reassuring regarding the lymph node status. In our series, we found thirteen patients (30.2%) with adenomegaly, ten of whom had undergone nephrectomy and histopathological analysis, which showed six patients with completely resected tumors (i.e., stage I and II) and four patients with incompletely resected tumors (i.e., stage III and IV), and the difference was statistically insignificant ($p=0.609$), justifying that any adenomegaly does not mean tumor invasion. In the literature, liver metastases are much rarer [10]. KADRI N. et al in Morocco in 2021 [37], found three patients with liver metastases out of thirteen metastatic patients, i.e. a proportion of 23%. These three cases had simultaneous metastases in the lung. MOULOT MO et al [19] in Ivory Coast 2018 had found metastatic cases in 18.6% ($n = 10$). The metastases were localized only to the lungs in 8 patients and to the liver in one patient. Simultaneous metastatic localization of liver and lung was found in one patient, i.e., liver localization in 20% (2 cases). In our series, we found patients with metastases in 17.7%, i.e. eight patients. Metastases were localized only to the lungs in five patients and to the liver in two patients. The simultaneous localization of the liver and the lung in one patient, i.e. a hepatic localization in 37.5% of the metastatic patients, this high rate of hepatic metastases could be justified by the late discovery of the tumor. In our series, abdomino-pelvic ultrasound was performed in 95.6%, i.e. 43 patients out of 45. The other two cases were included in the study because they had undergone an abdominal CT scan; the reason for the absence of an ultrasound report could be justified by its loss in the file on the one hand, and on the other hand, the non-performance of an ultrasound scan could be an exorbitant expense for the parents when the child had already undergone a scan. The CT scan was performed in nine patients (20%); this low rate did not allow us to compare the results of the ultrasound with those of the CT scan; the chest X-ray was performed in all patients (100%) to look for pulmonary metastases. In this study, 64.4% ($n=29$) of patients had undergone histological analysis after extended nephrectomy. All patients had benefited from histology in the studies conducted by LAIGLE V and MOLUA [1,2]. This low rate of histology in our series could be explained by the lack of financial means for some parents, the absence of surgery for some patients, the non-availability of the histological report in the patient's file and death before a possible nephrectomy. However, this cohort remains representative with figures usually described, with a clear predominance of nephroblastoma, representing 93.1% (27 cases) in this series, the figures in the literature range from 87 to 93% [1,2,10,23]. The proportion of non-nephroblastoma tumors represented 6.9% (2 cases) including; a mesoblastic nephroma and an inflammatory mass. This low rate did not allow us to statistically analyze the performance of imaging in the diagnosis of nephroblastoma. BOUZHIR M. A et al [21] and KADRI N. et al [26] note a predominance of tumors of intermediate risk respectively of 83.3% and 45%. This corroborates with our study which shows a large majority of intermediate risk tumors at 85.7% whereas FOFANA N.S et al [22] found 62.5% of high risk tumors. This difference could be explained by the fact that in the latter study only metastatic nephroblastomas were concerned. Concerning the ultrasonographic characteristics of the renal tumors according to the clinico-pathological stage; the right localization, regular tumor contours and the spur sign were more associated with tumors with complete resection whereas the left localization, irregular contours as well as intra-tumoral calcifications were associated with tumors with incomplete resection with statistically significant analyses for laterality ($p=0.021$), contours ($p=0.014$), calcifications ($p=0.001$). The spur sign did not show a statistically significant analysis ($p=0.132$) but there were eight cases or 50% of tumors with complete resection against 2 cases or 20% of tumors with incomplete resection. Elements such as reflux without invasion of neighbouring structures and pleural effusion argued in favour of an incompletely resected tumour but were not statistically significant ($p=0.092$ and $p=0.142$). However, these results are taken with reservation, as we intend to carry out a study with a larger sample to confirm or refute

these data. Regarding the limitations of this study, it should be noted that its retrospective nature, the lack of systematic histopathological analysis in all patients, the low rate of CT scan and the lack of nephrectomy in some patients were the main limitations of this study. As strengths: the present series is a first study carried out in our setting and having used cross-sectional imaging (US and CT). **CONCLUSION:** This study, which aimed to establish the radio-clinical occurrence of nephroblastoma managed at the CUK, allowed us to make the following observations: children of both sexes aged less than 5 years are the most affected. The majority of children referred for abdominal distension, in whom the physical examination shows a mass on palpation with a lumbar contact. Ultrasonographic examination was the most commonly used imaging technique in the hospital setting of Kinshasa for diagnosis and follow-up with good correlation to histopathological findings. The rate of CT scan remains low in our environment and the chest X-ray still retains its importance, as elsewhere, in the assessment of extension in search of pulmonary metastases. In view of the above, ultrasonography represents the imaging means adapted to the socio-economic conditions of our population for the initial diagnosis, the assessment of locoregional extension as well as the follow-up of children who have undergone chemotherapy and surgery. In conclusion, these data corroborate the majority of the data in the literature. Protection of Human and Animal: Rights The authors declare that this study did not involve experiments on patients, subjects, or animals. Confidentiality of Data: The authors declare that this study does not contain any personal data that could identify the patient or subject. Funding of the Study This study did not receive specific funding from any public or private institution. *Funding of the Study:* This study did not receive specific funding from any public or private institution. Conflict of Interest Statement: All the authors do not have any possible conflicts of interest. Contribution and Responsibility of the Authors: 1. Dr. Frederick Tshibusu Tshienda: writing and proofreading. 2. Oscar Mokambo Eputa: writing and proofreading, 3. Nina Doma Nsimba: proofreading 4. Aléine Budiongo Nzazi : proofreading , 5. Angèle Mbongo Tanzania¹: proofreading, 6. François Beya Kabongo: writing and proofreading, 7. Karim Assani: proofreading. 8. Gueth Kundabi Akoto: proofreading. 9. Damien Kamate Kiraulu : proofreading. 10. Valentin Kazadi Tshipamba: proofreading , 10. Theo Mbala Biayi: proofreading, 11. Nestor Ntumba Kabeya: proofreading, 12. Idesbald Mwepu : proofreading , 13. Jean-Pierre Bungu Kalala: proofreading, 14. Benjamin Kabwe Mwilambwe: proofreading , 15. Gertrude Luyeye Mvila, 16. Jean Mukaya Tshibola: proofreading 17. Joseph Bodi Mabiala: proofreading , 18. Michel Lelo Tshikwela proofreading , 19. Bienvenu Lebwaze Massamba: proofreading , 20. Jean Lambert Gini Ehungu: proofreading , 21. Antoine Molua Aundu: proofreading, 22. René Ngiyulu Makwala : proofreading. Tables and figures: table 1. distribution of patients according to clinico-biological parameters, table 2. distribution of according to ultrasonographic parameters, CT and locoregional extension, table 3. distribution of tumors according to histological type and tumor risk, table 4. Ultrasonographic characteristics according to clinicopathological stages and tumor extension according to stage. Figure 1: Distribution of children according to age, Figure 2: Distribution of patients according to sex (A) and according to the realization or not of echography (B), Figure 3: Distribution of cases without and with pulmonary metastasis (A) and Distribution of tumor staging (B). Figure 4: Initial examination before chemotherapy in a male patient, 3 years old, with a left renal endo and exo mass, compatible with a ruptured nephroblastoma .Figure 5: Abdominopelvic ultrasound after 6 courses of chemotherapy in the same 3 year old patient with a ruptured left renal nephroblastoma .Figure 6: 7 year old patient with normal renal ultrasonography. Figure 7: Pre-therapeutic abdominopelvic ultrasound in a 4 year old patient with left ruptured renal nephroblastoma. **References:** 1. Molua A. Contribution of radiology in the diagnosis of nephroblastoma. 1996. 2. Laigle V, Querat. CT scan of renal tumors in children managed according to the SIOP protocol, Nantes retrospective study of 62 cases over 10 years. <https://www.archive.bu.univ.nantes.fr>. 3. Collins A, Demarche M, Dresse MF, Forget P, Lombet J, Jamblin P, et al. [Renal tumors in children. A single center study of 31 cases]. Rev Med Liege. 2009;64(11):552-559. 4. Weidner M-A. How to shorten the diagnostic delay of cancer in children and adolescents. Proposed means of awareness. 2015; not reported. 5. Tahri A, Bencheikroun N, Karkouri M, Dahami Z, Sahraoui S, Acharki A, et al. Adult nephroblastoma. About three cases. Annales d'Urologie. 2001;35(5):257-261. 6. Haouas N, Sahraoui W, Sridi K. Nephroblastoma of the adult. Progress in Urology. 2005;3. 7. Gombé M C, Godet J, Magueye G S. Cancers in Francophone Africa. <https://www.iccp-portal.org/system/files/resources/LivreCancer.pdf>. 8. Axt J, Abdallah F, Axt M, Githanga J, Hansen E, Lessan J, et al. Wilms tumor survival in Kenya. J Pediatr Surg. 2013;48(6):1254-1262. 9. Doumbia AK, Togo P, Fousseyni T. Management of nephroblastoma in Bamako: about 18 cases. 3. 10. Desvignes C, Gorincour G, Coze C, Aschero A, Bourlière-Najean B, Colavolpe N. Kidney and excretory

tract tumors in children. EM-Consult. 2013;13. 11. Bianda NB, Kazadi M, Mputu-Yamba JB. Profile of abdominal masses in children and adolescents in Kinshasa. Congo med. 1993;484-488. 12. Luntala M. Elements of approach for the ideal treatment of Wilms' tumor at the University Clinics of Kinshasa. Specialization thesis in surgery. 1982. 13. Kongolo K.: Problematic of the treatment of nephroblastoma at the University Clinics of Kinshasa. Dissertation for specialization in Surgery. 1990. 14. Palangi M. Profil épidémiologique et anatomoclinique des tumeurs malignes solides de l'enfant Zaïrois, Mémoire de spécialisation en anatomie pathologique. 1987. 15. Kazadi M. Abdominal masses in children and adolescents at the University Clinics of Kinshasa. 1994. 16. Management of Pediatric Cancers at the University Clinics of Kinshasa. Service d'hémo-Oncologie Pédiatrique/CUK/October. 2019. 17. DIAKITE F. et al. Nephroblastoma: Epidemiological and therapeutic aspects at Donka Hospital in Conakry from 2007 to 2012. Rev int sc med Abj -RISM. 2019;21(1):50-53. 18. Atanda AT, Anyanwu L-JC, Atanda OJ, Mohammad AM, Abdullahi LB, Farinyaro AU. Wilms' tumour: Determinants of prognosis in an African setting. Afr J Paediatr Surg. 2015;12(3):171-176. 19. Moulot MO, Ehua M, Agbara K, Kopoin J, Coulibaly D, Yao K. Nephroblastoma in pediatric surgery at chu de treichville (abidjan - cote d'ivoire). J afr chir ped. 2018;1(2):412-417. 20. KANTE A. et al. Nephroblastoma in mali: about a follow-up of 40 cases, 2017. 21. Bouzahir M. Clinical, para-clinical, epidemiological and therapeutic aspects of nephroblastoma. 2021.22. Fofana N. Metastatic nephroblastoma at the pediatric oncology unit of CHU Gabriel Touré: clinical, radiological, therapeutic and evolutionary aspects. 2012. 23. Rouzic M-AL. Concordance between clinico-radiological signs of suspected nephroblastoma tumor rupture at diagnosis and post-chemotherapy histological analysis: consequences on therapeutic choice about a monocentric series from the Nancy CHRU. 107. 24. Roux C. Molecular classification of Wilms' Tumors by RNA-Seq analysis. 2020. 25. Zrig A. et al. Semiological characteristics of nephroblastomas on imaging. 2014;601. 26. Kadrin. Management of Nephroblastoma in the HOP department of Marrakech. 2021.

TABLES AND FIGURES

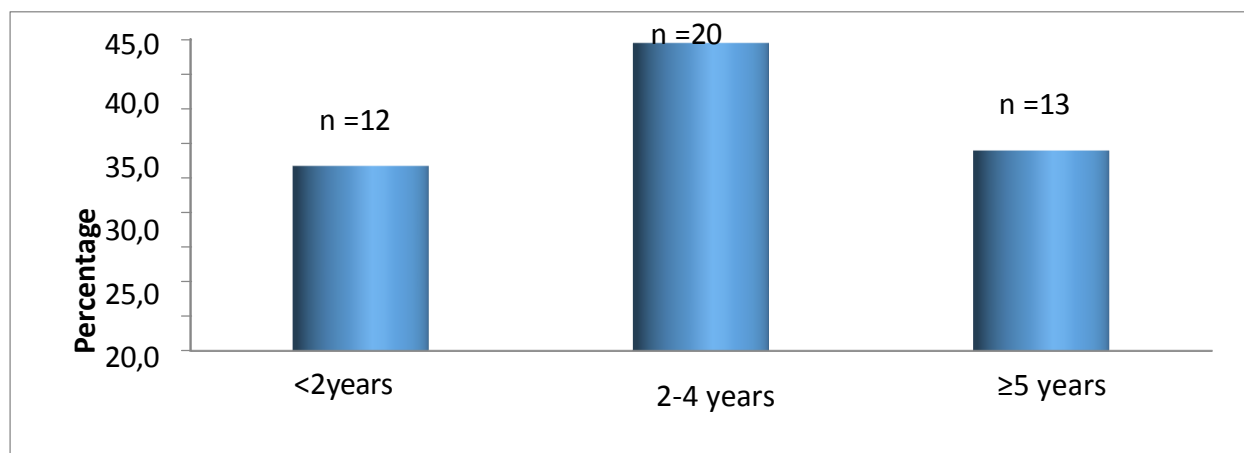


Figure 1. distribution of children by age

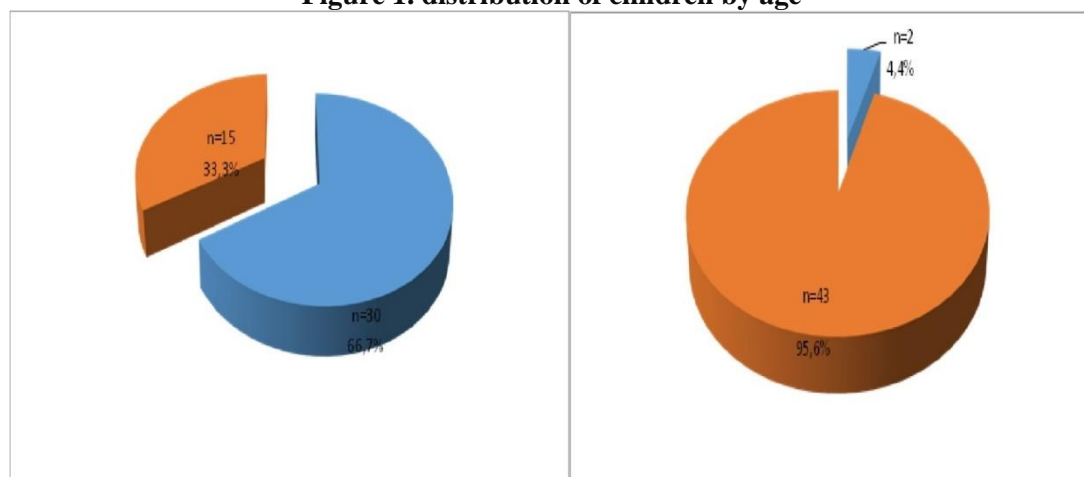


Figure 2: Distribution of patients according to gender (A) and whether or not ultrasound was performed (B)

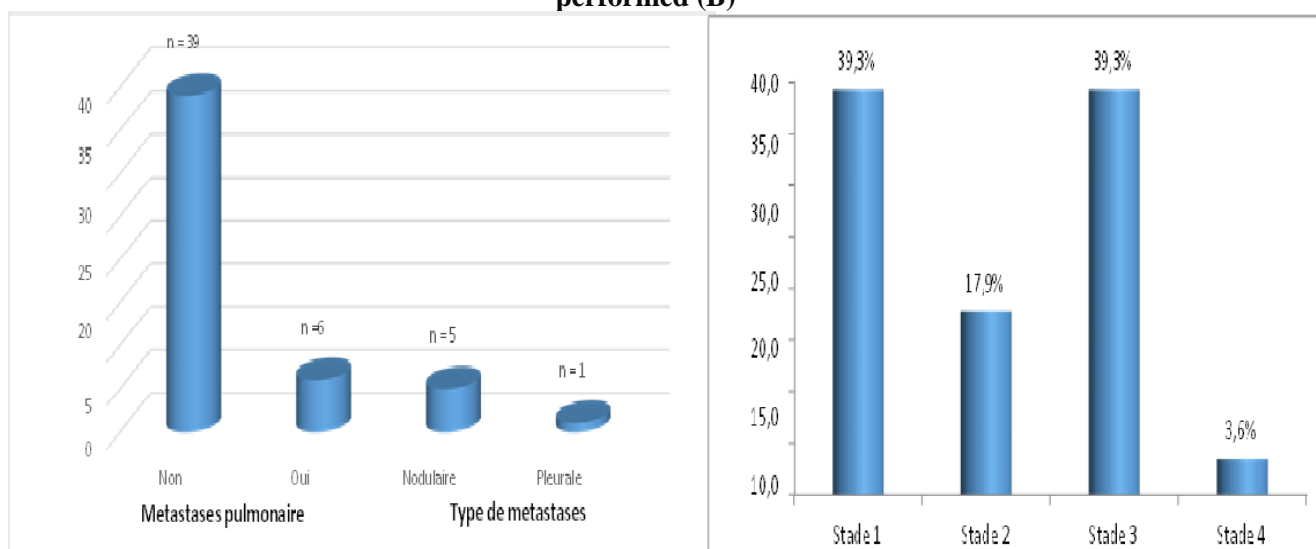


Figure 3. distribution of cases without and with lung metastases (A) and distribution of tumor staging (B).

Table 1. Distribution of patients according to clinico-biological parameters

Parameters	Whole group n=45	Male n=30	Female n=15	P
Abdominal distension	32(71,1)	22(73,3)	10(66,7)	0,447
Palpated abdominal mass	16(35,6)	11(36,7)	5(33,3)	0,548
Hematuria	11(24,4)	6(20,0)	5(33,3)	0,266
Abdominal pain	14(31,1)	9(30,0)	5(33,3)	0,539
General signs	20(44,4)	14(46,7)	6(40,0)	0,460
Digestive disorder	1(2,2)	0(0,0)	1(6,7)	-
Notion of trauma	1(2,2)	1(3,3)	0(0,0)	-
Urea (mg/dl)	20,8(13,4-27,1)	20,5(11,9-29,3)	21,0(10,2-28,0)	0,664
Créatinine(mg/dl)	0,60(0,45-0,70)	0,59(0,40-0,70)	0,60(0,40-0,70)	0,311
Hb(g/dl)	8,5±1,9	8,8±1,9	8,9±2,0	0,879

Table 2. Distribution according to ultrasonographic parameters, CT and locoregional extension

Variables	Whole group n=43(%)	Male n=28(%)	Female n=15(%)	P
○ Ultrasonographic parameters				
Location of the tumor				0,666
Right kidney	19(44,2)	13(46,4)	6(40,0)	
Left kidney	22(51,2)	13(46,4)	9(60,0)	
Bilateral	2(4,7)	2(7,1)	0(0,0)	

Echostructure				0,287
Solid (heterogeneous)	24(55,8)	17(60,7)	7(46,7)	
Mixed (necrotic-cyst.)	19(44,2)	11(39,3)	8(53,3)	
Flight point				0,592
Superior pole	19(44,2)	12(42,9)	7(46,7)	
Lower pole	11(25,6)	7(25,0)	4(26,7)	
Medialkidney	1(2,3)	0(0,0)	1(6,7)	
Toto kidney	12(27,9)	9(32,1)	3(20,0)	
Tumor volume	985(665-1196)	882,8(623-1501)	1026(491-1609)	0,427
Spur sign	12(27,9)	7(25,0)	5(33,3)	0,406
Contours				0,249
Irregular	30(69,8)	21(75,0)	9(60,0)	
Regular	13(30,2)	7(25,0)	6(40,0)	
Presence of tumor capsule	18(41,9)	9(32,1)	9(60,0)	0,079
Tumor rupture	3(7,0)	3(10,7)	0(0,0)	-
Backflowcavities	4(9,3)	1(3,6)	3(20,0)	0,114
Pyelocalcic				
Echogenicity				0,037
Hypoechoenic	23(53,5)	12(42,9)	11(73,3)	
Hyperechogenic	12(27,9)	9(32,1)	3(20,0)	
Isoechoenic	8(18,6)	7(25,0)	1(6,7)	
Calcifications	9(20,9)	7(25,0)	2(13,3)	0,315
HypertrophyCompensator	4(9,3)	2(7,1)	2(13,3)	0,436
Vascularization	17(39,5)	13(46,4)	4(26,7)	0,175
○ ParametersCT scan				
Size of the tumor (ml)	560(313,9-735,0)	560,6(1,0-560,6)	575(129,5-735,0)	
Spur sign	4	3	1	
Tumor capsule	2	0	2	
Tumor homogeneity				
Heterogeneous	3	1	2	
Homogenous	5	4	1	
Mixed	1	0	1	
Raising	6	4	2	
GreaseInfiltrate	1	0	1	
Crossing the line	1	0	1	
Median				
Pathological ganglion	1	0	1	
Intraperitoneal effusion	1	1	0	
Lung metastasis	1	1	0	
○ Locoregional tumor extension				
Trans median extension	7(16,3)	5(17,9)	2(13,3)	0,320

Repression without invasion	17(39,5)	12(42,9)	5(33,3)	0,392
Intraperitoneal effusion	5(11,6)	2(7,1)	3(20,0)	0,405
Satellite nodule	1(2,3)	0(0,0)	1(6,7)	-
Presence of thrombus	12(27,9)	11(39,2)	1(6,6)	0,315
Renalvein	5(11,6)	5(17,9)	0(0,0)	-
Inferior vena cava	7(16,3)	6(21,4)	1(6,7)	0,212
Presence of adenomegaly	13(30,2)	10(35,7)	3(20,0)	0,238
Hepaticmetastasis	3(7,0)	2(7,1)	1(6,7)	0,725

Table 3. Distribution of tumors by histological type and tumor risk

Variables	actualnumbe r	Percentage
○ Histological type of tumors		
Mixed type nephroblastoma	16	55,2
Nephroblastoma, stromal type	3	10,3
Nephroblastoma, regressive type	3	10,3
Nephroblastoma blastematous type	2	-
Nephroblastoma epithelial type	2	-
Inflammatory mass	1	-
Partially cystic differentiated nephroblastoma	1	-
Mesoblasticnephroma	1	-
Total	29	100,0
○ Tumor risk		
Intermediate Risk		85,8
High risk		7,1
Low risk		7,1
Total		100

Table 4. Ultrasonographic characteristics according to clinicopathological stages and tumor extension according to stage.

Variables	Total resection tumor n=16	Incompletely resected P tumor n=10	P
○ Clinical- pathological stages			
Tumor location			0,021
Right kidney	11(68,8)	2(20,0)	
Leftkidney	5(31,3)	8(80,0)	

Echostructure			0,412
Solid	10(62,5)	5(50,0)	
Mixed	6(37,5)	5(50,0)	
Flight point			0,503
Superior pole	9(56,3)	4(40,0)	
Lower pole	5(31,3)	3(30,0)	
kidney toto	2(12,5)	3(20,0)	
Spur sign	8(50,0)	2(20,0)	0,132
Contours			0,014
Irregular	7(43,8)	7(70,0)	
Regular	9(56,3)	3(30,0)	
Presence of the tumor capsule	8(50,0)	5(50,0)	0,656
Tumor rupture (suspicion)	0(0,0)	1(10,0)	
PC cavitydischarge	0(0,0)	1(10,0)	
Echogenicity			0,266
Hypoechoogenic	11(68,8)	7(70,0)	
Hyperechoogenic	2(12,5)	3(30,0)	
Isoechoogenic	3(18,8)	0(0,0)	
Necrosis	9(56,3)	6(60,0)	0,588
Hemorrhage	2(12,5)	0(0,0)	
Calcifications	1(6,9)	7(70,0)	0,001
Hypertrophy compensatory	1(6,3)	2(20,0)	0,323
Vascularization	6(37,5)	3(30,0)	0,517
○ Tumor extension according to stage			
Transmedian extension	2(12,5)	3(30,0)	0,274
Repression without invasion	6(37,5)	7(70,0)	0,092
intraperitoneal effusion	1(6,3)	3(30,0)	0,142
Satellitenodule	0(0,0)	1(10,0)	
Presence of thrombus	4(25,0)	1(10,0)	0,343
Renalvein	2(12,5)	1(10,0)	0,677
inferior vena cava	2(12,5)	1(10,0)	0,677
Proximal segment	0(0,0)	1(10,0)	-
Presence of adenomegaly	6(37,5)	4(40,0)	0,609
Hepaticmetastasis	0(0,0)	2(20,0)	-

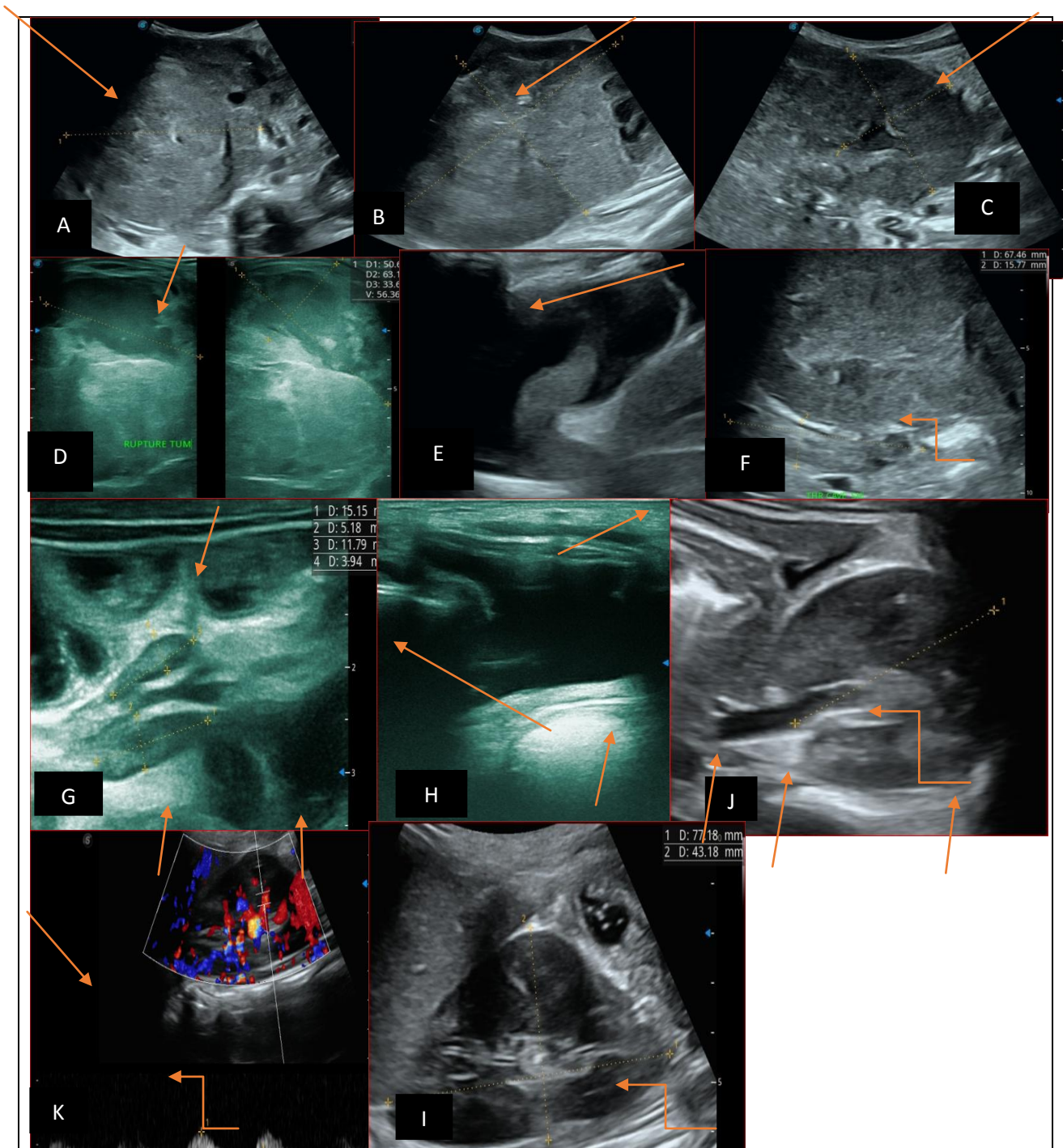


Figure 4: Initial examination prior to chemotherapy in a 3-year-old male patient with a left endo- and exo-renal mass compatible with ruptured nephroblastoma. Images A and B: represent a solid mass, endo and exo renal, left, with superior medio-polar flight point, hyperechogenic, heterogeneous, dotted with small empty echo areas. Image C: represents the healthy renal parenchyma located at the inferior pole, realizing the spur-like aspect. Image D: shows a hematic collection on tumor rupture Images E and F: show a thrombotic impregnation of the left renal venous and cava Images G : show a free ascites of medium abundance Image k: shows mesenteric adenopathies. Images H I: represent the

right kidney in B mode which is of normal echostructure. Image L: represents the right kidney with normal echostructure in triplex mode. Dr Frederick Tshibas Tshienda database.

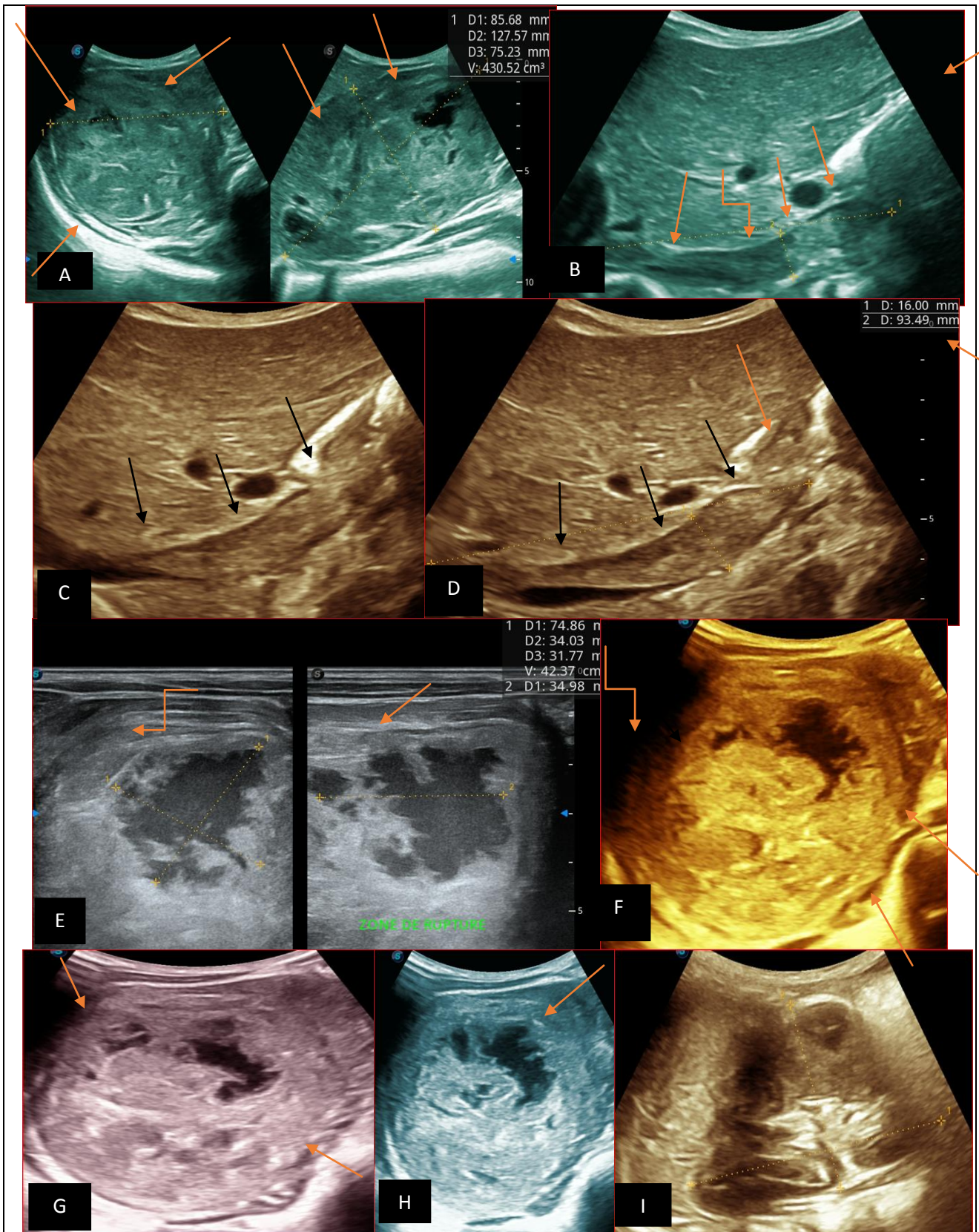


Figure 5: Abdominopelvic ultrasound check-up after 6 courses of chemotherapy in the same 5-year-old

patient with a ruptured left renal nephroblastoma; Images A, F, G and H : show a regression of the solid mass, endo and exo renal, left of the nephroblastoma treated by 6 courses of chemotherapy (current volume 430 ml vs) Images: B, C and: show a persistence of the thrombotic impregnation pan vena cava and renal ipsilateral. Image E: shows a volumetric regression of the intra-lesional hematic collection, on tumor rupture estimated 34.49 ml VS , Image I: represents the right kidney in B mode which is of normal echostructure. source: Dr Frederick Tshibusu Tshienda database.

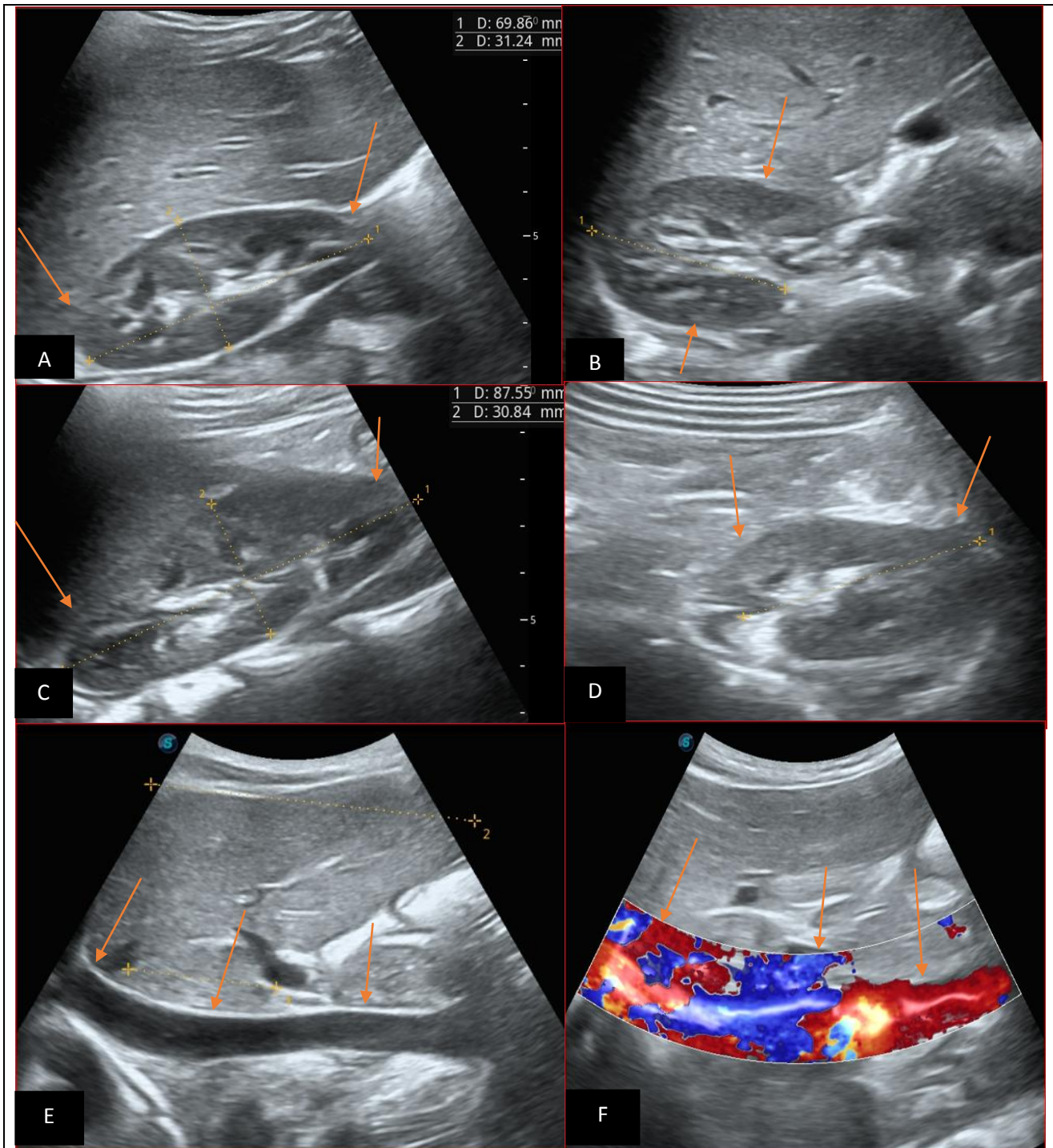
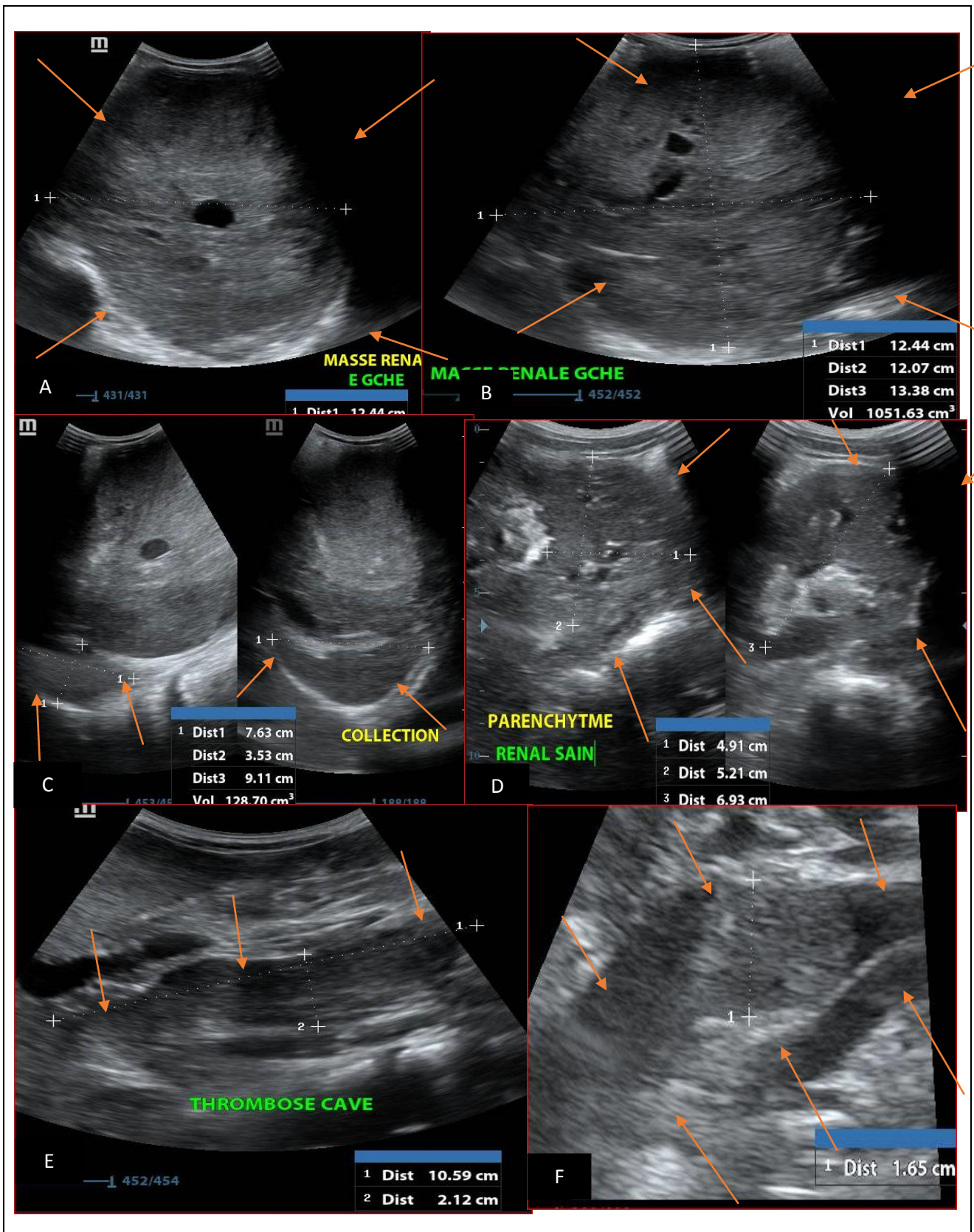


Figure 6: 7 year old patient with a normal renal ultrasonographic examination
Images A and B : represent a right kidney in B mode, morphologically normal
Images C and D: represent a morphologically normal left kidney
Images E and F; represent a normal permeability of the supra and retro hepatic cava segments in B mode
(E) and color doppler (F). source: Dr Frederick Tshibusu Tshienda database.



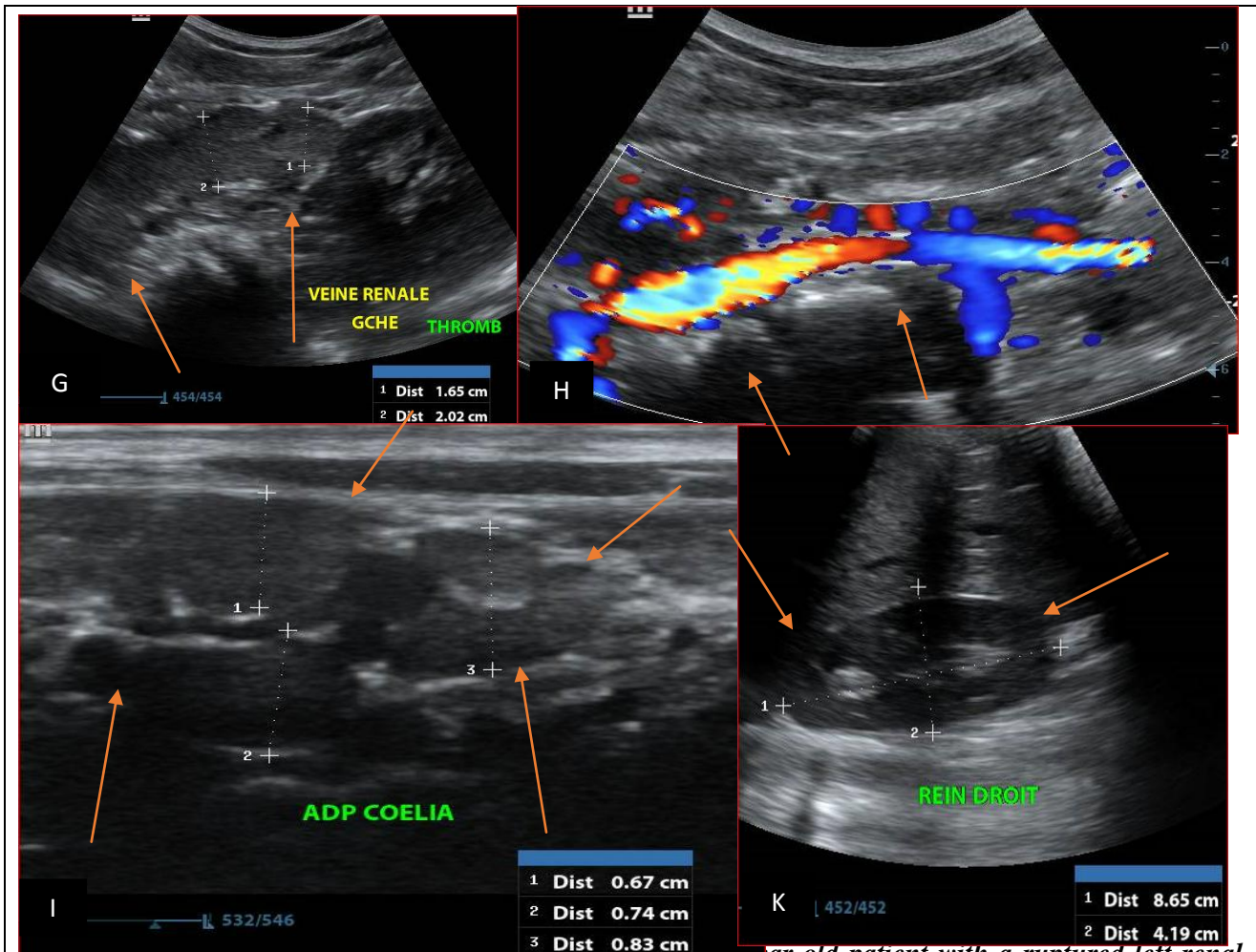
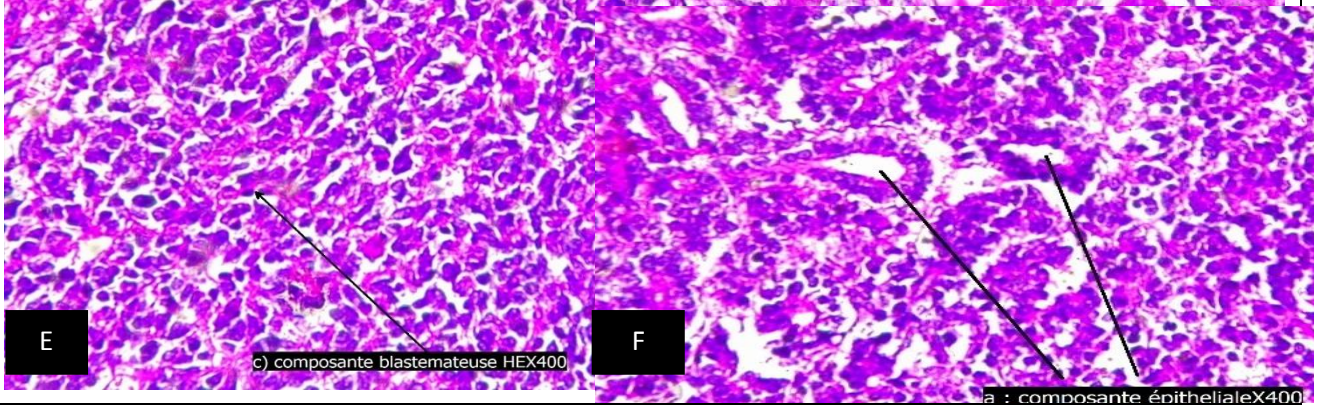
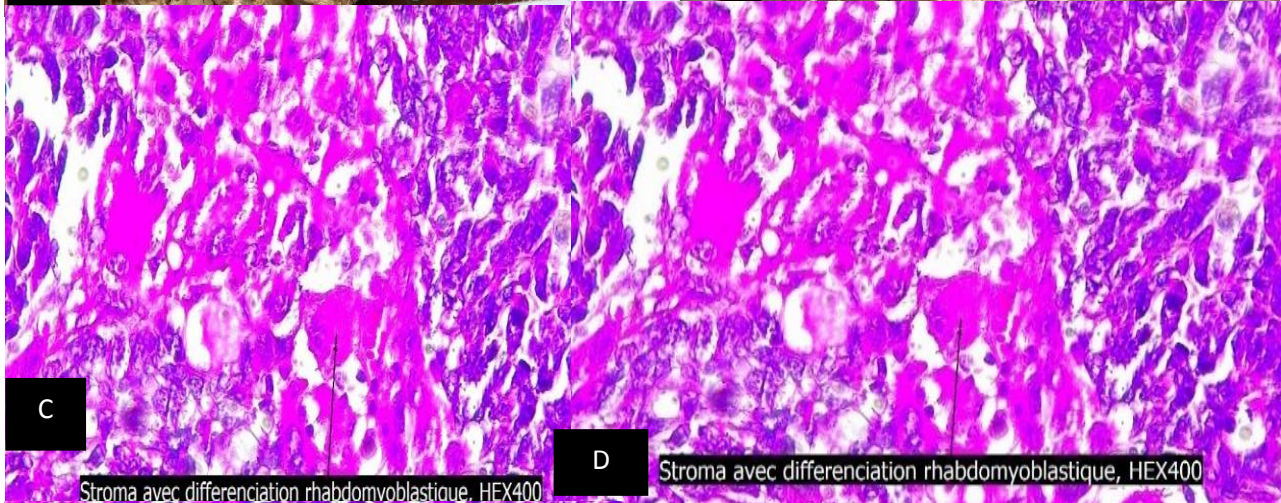
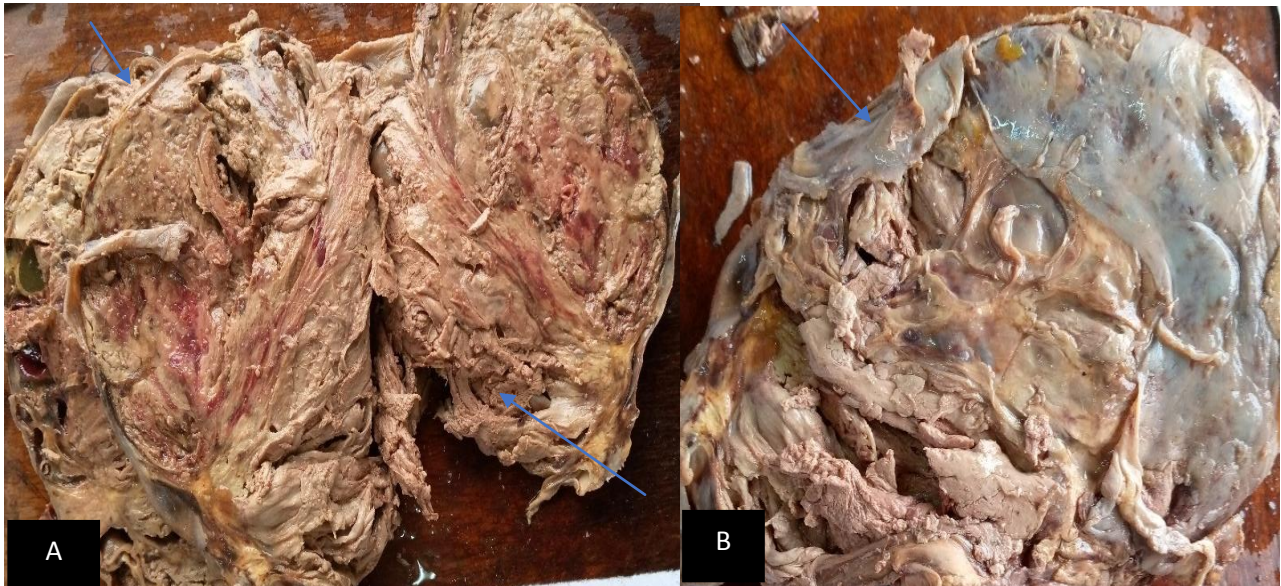


Figure 7: Pre-intraoperative abdominopelvic ultrasound in a 4-year-old patient with a ruptured left renal nephroblastoma; Images A and B: showing a solid mass, endo and exo renal left, dotted with necrotic-cystic areas, estimated at 1051.53 ml. Image C: shows a hematic echogenic collection of 128.7 ml, on tumor rupture. Image D: represents the healthy renal stump, located at the inferior polar level. Image E-F-G: represent an echogenic thrombotic impregnation of the ipsilateral renal and vena cava. Image H: image in color Doppler mode, representing a normal permeability of the aorta. Image I: represents multiple hypoechoic coelio-mesenteric adenopathies. Image K: represents the right kidney in B mode, which is of normal echostructure. source: radiodiagnostic and medical imaging department of the university clinics of kinshasa.



Figure 8: Abdominopelvic CT scan of a 5-year-old patient with a right renal nephroblastoma: Images A: showing a solid mass, endo and exo renal right, slightly enhancing after injection of contrast medium and a left kidney enhancing normally without mass syndrome. Images B: CT section through the kidneys,

showing a hypoechogenic right renal mass, with the spur sign (two arrows), Image C: large solid mass, endo and exo-right renal, moderately heterogeneously enhancing after iodinated contrast medium impregnation, Image D: CT section passing through the lower abdominal stage, showing the digestive tract slightly depressed on the left, images E and F: CT sections passing through the mediastinal stage, showing a symmetry of four cardiac cavities well opacified after impregnation with contrast medium. source: Dr Frederick Tshibusu Tshienda database.



Anatomopathological analysis of our patients with nephroblastoma. Images A: Anatomopathological morphological image after macroscopic analysis, showing the section slices of a nephroblastoma largely necrotic. Images B: Morphological anatomopathological image after macroscopic analysis, showing a Nephroblastoma with rupture of the capsule (arrow). Images C-E: Microscopic anatomopathological image of the Nephroblastoma HE X 400, showing a stroma with rhabdomyoblastic differentiation, HEX400. Images D: Microscopic anatomopathological image of the Nephroblastoma HE X 400, showing an epithelioid component, HEX400. Image F : anatomopathological microscopic image of Nephroblastoma HE X 400, showing a blastematos component, HEX400. sources: anatomopathology department of the university clinics of Kinshasa.